

Elastic Constants of Ice III, V, and VI by Brillouin Spectroscopy

C. A. Tulk,^{*,†} H. Kiefte,[‡] and M. J. Clouter

Department of Physics and Physical Oceanography, Memorial University of Newfoundland,
St. John's, Newfoundland, Canada A1B 3X7

R. E. Gagnon

National Research Council of Canada/Institute for Marine Dynamics,
St. John's Newfoundland, Canada A1B 3T5

Received: October 11, 1996; In Final Form: January 24, 1997[⊗]

Large single crystals of ice III, ice V, and ice VI have been grown and *in situ* Brillouin spectra collected at various crystal orientations. The elastic constants have been calculated at $-20\text{ }^{\circ}\text{C}$ and 2.2 kbar, $-35\text{ }^{\circ}\text{C}$ and 3.0 kbar, and $-2\text{ }^{\circ}\text{C}$ and 7.2 kbar for ice III, ice V, and ice VI, respectively. The data were used to calculate the isotropic elastic constants of polycrystalline aggregates of each phase, and the results are compared with known polycrystalline data.

Introduction

Little is known regarding the physical properties of many of the high-pressure phases of ice. Perhaps the most likely explanation of this is due to difficulty of obtaining and studying large high-quality single crystals. This laboratory has recently completed studies leading to the elastic constants of three high-pressure phases of H_2O ice, namely, ice III,¹ ice V, and ice VI.² Large ($\sim 0.3\text{ cm}^3$) high-quality single crystals of each phase were grown, and *in situ* Brillouin spectra were collected at various crystal orientations through a complete 360° sample rotation about the laboratory z axis. This allows for accurate determination of the elastic constants. In all, three single crystals of ice III, three single crystals of ice V, and four single crystals of ice VI were studied up to ~ 8.5 kbar. In this paper we review the elastic properties of ice III and ice VI and present the elastic constants of ice V for the first time.

Single crystals usually exhibit acoustic anisotropy, and hence crystallographic symmetry naturally plays a large role in any accurate description of the elastic behavior of crystalline solids. The crystal structure of ice III has been determined to be tetragonal with the $P4_12_12$ space group and has six independent elastic constants. As in all the ice phases of the present study, the water molecules form distorted tetrahedrons.³ Dielectric properties of ice III in the range -24 to $-44\text{ }^{\circ}\text{C}$ and 2.4 to 3.4 kbar imply that ice III is disordered.⁴ Recent neutron diffraction studies indicate that ice III is, in fact, partially hydrogen ordered.⁵ The crystallographic structure of ice VI has been found, at high temperatures, to be tetragonal with the space group $P4_2/nmc$ and has six independent elastic constants.⁶ At low temperatures ice VI may transform to an orthorhombic structure.⁷ Ice VI was found to be disordered with respect to hydrogen atom positions by dielectric,² Raman,⁸ and infrared studies.⁹ The abnormally high density of ice VI is achieved through the formation of two identical interpenetrating sublattices in which the molecules of one lattice fill the voids of the other. The molecules within each lattice form a hydrogen-bonded framework, but there are no such bonds connecting the

interpenetrating lattices. This has been called a "self-clathrate" by Kamb.³ The crystal structure of ice V was shown to be monoclinic,⁶ which is the lowest symmetry of the known high-pressure phases of ice. The space group has been shown to be $A2/a$, with 28 molecules per unit cell and an angle of monoclinicity of 109.2° . There are six independent elastic constants required to completely describe the elastic properties of ice III and ice VI, and there are 13 independent elastic constants required to completely describe the elastic properties of ice V.¹⁰

Recently, there have been several molecular dynamic and *ab initio* studies of the high-pressure crystalline and amorphous phases of ice and water clusters using a variety of interaction potentials.^{11–16} Of particular note are molecular dynamics calculations simulating the pressure-induced phase transformation from ice Ih to high-density amorphous ice by application of pressure at liquid nitrogen temperatures.^{17,18} The elastic constants of ice Ih were calculated at the transition temperature and pressure of 80 K and 10 kbar, respectively. It was indicated that the transition may be driven by a violation of the Born criteria for mechanical stability. Intermolecular potentials and intermolecular dynamics of various phases of ice are still poorly understood. Experimental data for the elastic constants properties are limited, and very little data have been collected from single-crystal crystal samples. Ultrasonic¹⁹ and Brillouin spectroscopic techniques^{20–23} have, however, been used to determine the average acoustic velocity and bulk modulus of polycrystalline samples and very small single crystals above 10 kbar. These results will be compared with the present results. Values for the elastic constants of ice, while of fundamental importance, provide a sensitive test for potentials which model the hydrogen bond in both the water ice system and other related substances.

Experimental Method and Crystal Growth

In Brillouin spectroscopy light is scattered inelastically from acoustic phonons through the elastooptic effect. This results in a Doppler shift of the frequency of the incident light which is directly related (through the Brillouin equation) to the velocity of the scattering acoustic phonon. The velocity of acoustic phonons in anisotropic solids may be described by plane wave solutions of the equation of motion of an elemental volume. Such solutions lead directly to expressions for the velocities of

* To whom correspondence should be addressed.

[†] Present address: Steacie Institute for Molecular Sciences, National Research Council of Canada, Ottawa, Ontario, Canada K1A 0R6.

[‡] Deceased.

[⊗] Abstract published in *Advance ACS Abstracts*, June 15, 1997.

the two transverse and one longitudinal acoustic waves in terms of the appropriate elastic constants, density, and the direction of wave propagation within the crystal. The elastic constants are then determined by least-squares fitting (χ^2 minimization) the elastic constant parameters of the expressions to the experimental Brillouin frequency shift data for various crystallographic directions in the ice samples. Excellent reviews are given by Stoicheff²⁴ and by Benedick and Fritsch.²⁵

In the present study an argon ion laser, in single mode operation, provided monochromatic laser light of 514.5 nm wavelength at power levels of about 35 mW. The laser beam was focused and entered the bottom optical port of the high-pressure chamber and then passed through the sample. The light scattered at 90° (defining the direction of propagation of the acoustic wave in the laboratory frame) was filtered through collection optics before entering a triple pass piezoelectrically scanned Fabry-Perot interferometer. Photons were detected using a photomultiplier tube with an amplifier discriminator and counted as a function of channel number using a data acquisition system.

The sample containment cell and experimental setup have been discussed in previous articles.²⁶ The high-pressure cell was made of a block, $7 \times 7 \times 10$ cm, of hardened 300 maraging steel with two orthogonal intersecting bores. One bore, parallel to the long axis, formed the high-pressure chamber, and the other, parallel to one of the short axes, was sealed with quartz windows and formed two optical viewing ports with a diameter of 1.8 mm. The top was sealed with a rotation stem which was connected to the sample holder in the pressure chamber. This enabled complete rotation of the sample about the laboratory z axis while under pressure. The hydraulic pressure transmitting fluid was a mixture of Monoplex (a transparent synthetic oil) and isopentane. Monoplex was used alone in the lower pressure ice III experiments; however, the oil froze at higher pressures and was subsequently mixed with isopentane to reduce the freezing temperature. The samples were isolated from the hydraulic oil by a thin silicone disk which served to prevent oil intrusion into the sample during crystal growth as well as to prevent the formation of clathrates (see for example ref 2).

Pressurization was achieved through the use of a 3 kbar Enerpac hand pump connected to a hydraulic intensifier which stepped up the pressure in a 1:16 ratio before entering the high-pressure chamber. The fluid filled the chamber, surrounded the ice specimen, and provided hydrostatic pressure. The glass sample containment cell, ~ 0.4 cm³, was coupled to the rotation stem by a brass tube.

The method used, to produce single crystals, was similar for all three phases studied. Briefly, triply distilled deionized water was boiled for several minutes to remove any dissolved gases and allowed to cool to room temperature under vacuum. The water was placed in the cell which was then placed in the high-pressure chamber at room temperature. The pressure was then increased to either ~ 3.3 , ~ 4.4 , or ~ 7.5 kbar for ice III, ice V, or ice VI, respectively. The temperature of a plexiglass cryostat containing the high-pressure cell was then reduced to ~ -35 °C, and after several hours nucleation occurred so that the sample completely froze directly into the desired phase within several seconds. Due to rapid freezing the grain size of the sample was of the order 100 nm³. The sample was viewed with the aid of a microscope and a video system. The temperature of the cryostat and polycrystalline sample were raised to ~ -12 °C in the case of ice III and ice V and to ~ 0.5 °C in the case of ice VI, and the sample was left to equilibrate for several hours. A slow and controlled melting process was initiated by

reducing the pressure to approximately 2.2, 2.9, and 6.7 kbar for ice III, ice V, and ice VI, respectively, thus barely crossing the phase boundary with liquid water. When only a small ice seed remained, the pressure was slightly increased to initiate a slow refreezing of the sample. This procedure rarely resulted in a single crystal, and the process would be repeated until a large high-quality single crystal suitable for Brillouin spectroscopy was obtained. Ice V single crystals were cooled, at ~ 3.0 kbar, to ~ -70 °C in an attempt to nucleate ice II. No such nucleation occurred, and ice V remained metastable at ~ -70 °C for several days, as determined by comparison of Brillouin frequency shift data with well-known values obtained from polycrystalline samples of both ice II and ice V.²⁰ The temperature was then raised, at constant pressure, to -35 °C, and the Brillouin frequency shift data presented in Figure 1 were collected.

Results

Two crystals of ice III provided a total of 149 frequency shift measurements at -20 °C and 2.2 kbar, three crystals of ice V provided a total of 200 frequency shift measurements at -35 °C and 3.0 kbar, and three crystals of ice VI provided 191 frequency shift measurements at -2 °C and 7.2 kbar. Other crystals of ice III and ice VI were grown and data collected for the purpose of studying the pressure dependence of the elastic constants, and the results will be fully discussed in a subsequent paper.

In the case ice III and ice VI a very good guess ($\pm 2^\circ$) of the Euler angles θ and ϕ relating the laboratory frame to the crystallographic frame was obtained by making use of the birefringence of optically uniaxial crystals. The remaining Euler angle χ was fitted to the frequency shift data along with the elastic constants. In determining θ and ϕ , the cryostat and high-pressure cell containing the sample were placed between rotatable crossed polaroid filters, and light from an unpolarized helium neon laser was passed through the samples. Rotating the filters about the y axis caused the light transmitted through the sample to become almost completely extinguished at the appropriate orientation. A simple expression describes the extinction angle in terms of the rotation of the crystal about the laboratory z axis ($\Delta\phi$) and the two Euler angles θ and ϕ . Extinction angles were measured at several crystal orientations, and the Euler angles were fitted to the experimental data using a least-squares routine. In the case of ice V such measurements were not feasible. Ice V is an optically biaxial crystal, and the Biot-Fresnel law describing the extinction points of such crystals leads to several indistinguishable choices of optic axes orientation. The problem is further complicated by the fact that the crystal axes of the monoclinic system are not orthogonal, and the relation between the optic axes and the crystal axes is not readily available. In the case of ice V the x_2 axis of the coordinate system in which elastic constant tensor is defined is parallel to the crystallographic b axis, and all the Euler angles were fitted with the elastic constants to the frequency shift data.

Values of the refractive index and densities are required in fitting the elastic constants to the Brillouin acoustic data. Density values of several ice phases have been obtained as a function of pressure, at -35 °C, by Gagnon *et al.*²⁰ The density when calculated under the present experimental conditions is considered well within experimental error. The refractive index of ice at various pressures was determined by Polian and Grimsditch²¹ using a linear function of Eulerian strain and density. Polian and Grimsditch extrapolated the refractive index through two phases transitions; it has been shown that for ice VI at 10.5 kbar the measured and extrapolated values agree to

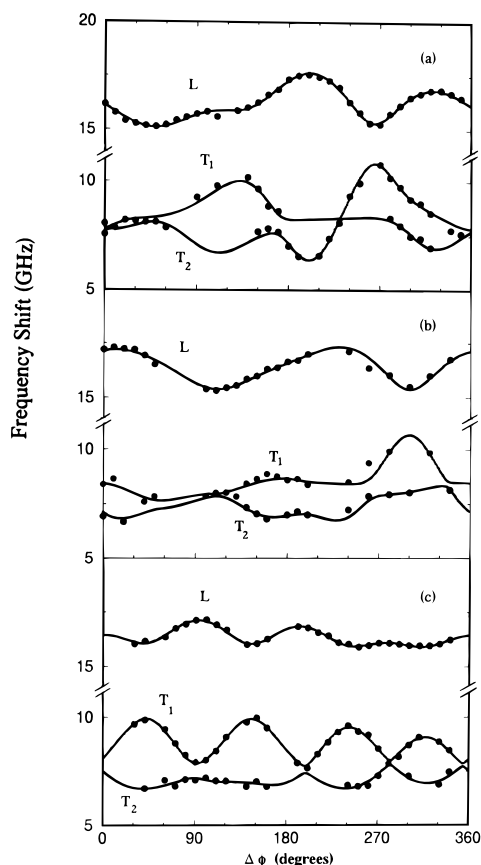


Figure 1. Ice V frequency shift data versus $\Delta\phi$. The Brillouin frequency shift data, solid circles, and calculated best fit curves, smooth lines: (a) crystal 1, (b) crystal 2, and (c) crystal 3. All data were collected at $-35\text{ }^{\circ}\text{C}$ and 3.0 kbar.

TABLE 1: Elastic Constants ($\times 10^4$ bar) of Ice III, Ice V, and Ice VI

	ice III ($P = 2.2$ kbar, $T = -20\text{ }^{\circ}\text{C}$)	ice VI ($P = 7.2$ kbar, $T = -2\text{ }^{\circ}\text{C}$)	ice V ($P = 3.0$ kbar, $T = -35\text{ }^{\circ}\text{C}$)
C_{11}	15.37 ± 0.5	26.84 ± 0.2	21.4 ± 1.2
C_{33}	11.55 ± 0.7	26.21 ± 0.2	19.3 ± 1.2
C_{44}	4.46 ± 0.2	6.31 ± 0.1	21.1 ± 1.3
C_{66}	5.68 ± 0.4	10.38 ± 0.1	7.5 ± 0.7
C_{12}	9.95 ± 0.6	14.52 ± 0.3	3.7 ± 0.5
C_{13}	6.51 ± 0.6	12.82 ± 0.2	7.5 ± 0.7
			C_{12} 12.2 ± 1.2
			C_{13} 9.5 ± 1.1
			C_{15} 0.17 ± 0.4
			C_{23} 11.8 ± 1.1
			C_{25} -0.1 ± 0.4
			C_{35} -0.3 ± 0.3
			C_{45} -2.1 ± 0.3

within 1%.²¹ The values for the ice phases studied in the present experiment have been calculated using their method, and their accuracy is considered to be comparable.

Plots of the Brillouin frequency shift versus change in Euler angle, $\Delta\phi$, for the three ice V single crystals are shown in Figure 1. The solid circles represent the experimental data points, and the smooth curves were calculated using the best fit elastic constants. Similar plots exist for ice III and ice V and have been reported previously.^{1,2} The fitting program was run on each crystal individually; the agreement between each independent system was found to be excellent. The best fit elastic constants for each phase are shown in Table 1. These have been determined by running the least-squares routine for all data from each phase combined. The errors quoted for the elastic constants of ice III and ice VI represent a standard deviation in

TABLE 2: Polycrystalline Elastic Properties of Ice III, V, and VI^a

	ice III ($P = 2.2$ kbar, $T = -20\text{ }^{\circ}\text{C}$)	ice V ($P = 3.0$ kbar, $T = -35\text{ }^{\circ}\text{C}$)	ice VI ($P = 7.2$ kbar, $T = -2\text{ }^{\circ}\text{C}$)
V_L (m/s)	3658 (3648)	4198 (4168)	4473 (4517)
V_T (m/s)	2008 (1882)	2164 (2186)	2272 (2316)
B_s (kbar)	92.7 (99.4)	143 (137)	177.7 (179.3)
μ (kbar)	46.7 (41.0)	58.9 (59.6)	69.9 (72.6)
λ (kbar)	61.5 (72.1)	103.7 (97.3)	131.1 (130.9)
E (kbar)	120.0 (108.1)	155.4 (156.2)	185.4 (191.9)
σ (kbar)	0.284 (0.319)	0.319 (0.310)	0.326 (0.321)

^a The values given in parentheses were calculated from experimental data collected from polycrystalline samples at 2.76 kbar and $-27.2\text{ }^{\circ}\text{C}$, 3.0 kbar and $-35\text{ }^{\circ}\text{C}$, 7.2 kbar and $-35\text{ }^{\circ}\text{C}$ for ice III, ice V, and ice VI, respectively.²⁰

the least-squares fit caused by uncertainties in the frequency shifts and crystal orientation. The errors for ice V represent a combination of the standard deviation error for each of the independent crystal systems. This was done to account for the variation in best fit elastic constants between each of the three ice V crystals studied. The variation is thought to be a result of the large number of parameters being fitted. There is an additional systematic error of $\sim 1\%$ due to uncertainties in the density, refractive index, and scattering angle.

Various elastic properties of isotropic polycrystalline ice aggregates have been derived using the elastic constants found in this study. For these calculations polycrystalline samples are assumed to consist of small grains randomly oriented, and grain boundaries are assumed to have no effect on the elastic properties of the aggregate. The average longitudinal acoustic velocity V_L was estimated by performing a simple average over 4π steradians. The bulk modulus, B_s , can be calculated from the elastic compliance constants following a method outlined by Nye.¹⁰ The Lamé constants μ and λ have been calculated from the Bulk modulus and the average longitudinal acoustic velocity using $B_s = \lambda + (2/3)\mu$ and $\mu = (3/4)(\rho V_L^2 - B_s)$. The values of Young's modulus and Poisson's ratio were determined using the respective expressions $E = \mu(3\lambda + 2\mu)/(\lambda + \mu)$ and $\sigma = \lambda/[2(\lambda + \mu)]$. The average shear velocity can be calculated from the shear modulus μ by $V_T = (\mu/\rho)^{1/2}$. The values calculated in the present study (see Table 2) are compared with those found directly from Brillouin acoustic measurements of polycrystalline samples,²⁰ which are listed in parentheses in Table 2. The agreement is quite good.

The elastic constants of ice VI also seem to increase with increasing pressure (up to at least 8.5 kbar); C_{11} has the greatest slope, except C_{44} which is nearly constant. The elastic constants of ice VI have also very recently been found by collecting Brillouin spectra from small single crystals in a diamond anvil cell at pressures above 10.5 kbar by Shimizu *et al.*²³ The present elastic constant results may be extrapolated to 12.3 kbar and compared with the results directly quoted in the paper of Shimizu *et al.* which are listed in parentheses in the following: $C_{11} = 31.9$ (32.8), $C_{12} = 18.14$ (11.8), $C_{13} = 15.66$ (14.7), $C_{33} = 30.38$ (27.8), $C_{44} = 6.12$ (6.12), and $C_{66} = 12.03$ (5.9) (all values in 10^4 bar). While there seems to be general agreement, the most noticeable difference is in C_{66} . It should be noted that the samples used in the study by Shimizu *et al.* were produced in a diamond anvil cell and are necessarily very small. It is quite likely that the elastic properties of such small samples may be subject to surface and other effects. In addition, the data appear to have been collected from only one sample.

In conclusion, knowledge of the elastic constants, while being a fundamental material property, may lead to better understanding of water in general by providing a sensitive test of

intermolecular potentials. The authors thank the Institute of Marine Dynamics of the National Research Council of Canada for providing the water samples.

References and Notes

- (1) Tulk, C. A.; Gagnon, R. E.; Keifte, H.; Clouter, M. H. *J. Chem. Phys.* **1994**, *101*, 2350.
- (2) Tulk, C. A.; Gagnon, R. E.; Keifte, H.; Clouter, M. J. *J. Chem. Phys.* **1996**, *104*, 7854.
- (3) Kamb, W. B.; Datta, S. K. *Nature (London)* **1960**, *87*, 140.
- (4) Wilson, G. L.; Chan, R. K.; Davidson, D. W.; Whalley, E. *J. Chem. Phys.* **1965**, *43*, 2384.
- (5) Londono, J. D.; Kuhs, W. F.; Finney, J. L. *J. Chem. Phys.* **1993**, *98*, 4878.
- (6) Kamb, B. *Science* **1965**, *150*, 205.
- (7) Kamb, B. *Trans. Am. Cryst. Assoc.* **1969**, *5*, 61.
- (8) Minceva-Sukarova, B.; Sherman, W. F.; Wilkinson, F. R. *J. Phys. Chem.* **1984**, *17*, 5833.
- (9) Whalley, E. In *Physics of Ice*; Pergamon: Oxford, 1965; pp 19–43.
- (10) Nye, J. F. In *Physical Properties of Crystals*; Oxford University Press: Oxford, 1972; pp 131–149.
- (11) Tse, J. S.; Klein, M. L.; McDonald, I. R. *J. Chem. Phys.* **1984**, *81*, 6124.
- (12) Yoon, B. J.; Morokuma, K.; Davidson, E. R. *J. Chem. Phys.* **1985**, *83*, 1223.
- (13) Ojamae, L.; Hermansson, K.; Dovesi, R.; Roetti, C.; Saunders, V. R. *J. Chem. Phys.* **1994**, *100*, 2128.
- (14) Lee, C.; Vanderbilt, D.; Laasonen, K.; Car, R.; Parrinello, M. *Phys. Rev. B* **1993**, *47*, 4863.
- (15) Impey, R. W.; Klein, M. L.; Tse, J. S. *J. Chem. Phys.* **1984**, *81*, 6406.
- (16) Bosma, W. B.; Fried, L. E.; Mukamel, S. *J. Chem. Phys.* **1993**, *98*, 4413.
- (17) Tse, J. *J. Chem. Phys.* **1992**, *96*, 5482.
- (18) Tse, J.; Klein, M. L. *J. Chem. Phys.* **1990**, *92*, 3992.
- (19) Shaw, G. H. *J. Chem. Phys.* **1986**, *84*, 5862.
- (20) Gagnon, R. E.; Kieifte, H.; Clouter, M. J.; Whalley, E. *J. Chem. Phys.* **1990**, *92*, 1909.
- (21) Polian, A.; Grimsditch, M. *Phys. Rev. B* **1983**, *27*, 6409.
- (22) Polian, A.; Grimsditch, M. *Phys. Rev. Lett.* **1984**, *52*, 1312.
- (23) Shimizu, H.; Nabetani, T.; Nishiba, T.; Sasaki, S. *Phys. Rev. B* **1996**, *53*, 6107.
- (24) Stoicheff, B. P. In *Rare Gas Solids*; Academic: New York, 1977.
- (25) Benedick, G. B.; Fritsch, K. K. *Phys. Rev.* **1966**, *149*, 647.
- (26) Gagnon, R. E.; Kieifte, H.; Clouter, M. J.; Whalley, E. *J. Chem. Phys.* **1988**, *89*, 4522.